

Interactive comment on “Improved simulation of precipitation in the tropics using a modified BMJ scheme in WRF model” by R. Fonseca et al.

Reply to comments by B. Samala (Referee):

1. In the 1-day and 4-month experiments we used a smaller domain for the purpose of testing different versions of the BMJ scheme. Once the best configuration of the scheme was found we used a tropical belt to check whether the improvements in the simulation of the observed precipitation were also seen in other tropical regions, in particular in the Western Hemisphere, and for both monsoon seasons. In the tropical belt experiments we decreased the resolution as we could not afford computationally a 24km horizontal resolution with this large domain.
2. We have used a tropical channel domain as we are interested in studying the Madden-Julian oscillation (MJO). In order to fully capture the MJO we need the whole tropics and sub-tropics given that in the boreal summer season it also exhibits northward propagation over Asia (Lee et al., 2013). Although running WRF in a tropical belt configuration is not very common, there are a few papers where the authors set up WRF in this way (e.g. Ray et al., 2011; Evan et al., 2013).
3. We have chosen the year of 2008 as, according to Ummenhofer et al. (2009), it was a neutral year with respect to both El Nino-Southern Oscillation (ENSO) and Indian Ocean Dipole (IOD). By choosing a neutral year we minimize the impact of climatic anomalies. We will make it clear in the paper why we chose this particular year for the model experiments.
4. We have only used CFSR data, downloaded from CISL RDA's website (<http://rda.ucar.edu/>), to generate initial and boundary conditions for WRF and we agree that if another dataset (or set of physics options) is used our modified BMJ scheme may not give such good results. However, with the information available in this paper users will know how to modify the BMJ scheme so that it gives a good estimate of the observed rainfall for the particular model configuration used.
5. We were not aware that the GFS data is now available at 25km resolution. We plan to perform higher resolution runs, with boundary conditions generated either from the output of a coarser grid or the new ERA-5 (~30km) re-analysis dataset, to be presented in a subsequent paper. However, there is always the question of whether a cumulus scheme should be used in those runs: e.g. Fujita et al. (2013) performed nested WRF experiments over the eastern Indian Ocean off Sumatra with 17.5km and 3.5km grids both run without a cumulus scheme while Evans and McCabe (2010) ran WRF over Southeastern Australia at 50km and 10km resolution with a cumulus scheme. For the horizontal resolutions used in the experiments discussed in this paper (24km and 30km) there is a general consensus that a cumulus scheme is needed.

References:

Evan, S., Rosenlof, K.H., Dudhia, J., Hassler, B. and Davis, S.M., 2013: The representation of the TTL in a tropical channel version of the WRF model. *Journal of Geophysical Research Atmospheres*, **118(7)**, 2835-2848, doi: 10.1002/jgrd.50288.

Evans, J.P. and McCabe, M.F., 2010: Regional climate simulation over Australia's Murray-Darling basin: A multitemporal assessment. *Journal of Geophysical Research*, **115**, D14114, doi: 10.1029/2010JD013816.

Fujita, M., Takahashi, H.G. and Hara, M., 2013: Diurnal cycle of precipitation over the eastern Indian Ocean off Sumatra Island during different phases of the Indian Ocean Dipole. *Atmospheric Science Letters*, **14**, 153-159, doi: 10.1002/asl2.432.

Lee, J.-Y., Wang, B., Wheeler, M.C., Fu, X., Waliser, D.E. and Kang, I.-S., 2013: Real-time multivariate indices for the boreal summer intraseasonal oscillation over the Asian summer monsoon region. *Climate Dynamics*, **40**, 493-509, doi: 10.1007/s00382-012-1544-4.

Ray, P., Zhang, C., Moncrieff, M.W., Dudhia, J., Caron, J.M., Leung, L.R. and Bruyere, C., 2011: Role of the atmospheric mean state on the initiation of the Madden-Julian oscillation in a tropical channel model. *Climate Dynamics*, **36**, 161-184, doi: 10.1007/s00382-010-0858-2.

Ummenhofer, C.C., England, M.H., McIntosh, P.C., Meyers, G.A., Pook, M.J., Risbey, J.S., Gupta, A.S. and Taschetto, A.S., 2009: What causes Southeast Australia's worst droughts? *Geophysical Research Letters*, **36(4)**, L04706, doi: 10.1029/2008GL036801.

Interactive comment on “Improved simulation of precipitation in the tropics using a modified BMJ scheme in WRF model” by R. Fonseca et al.

Reply to comments by Anonymous Referee #2:

However, the figures formatting needs improvement they are not clear.

We have made some improvements to the formatting of the figures.

We found out why the quality of the figures was not very good in the previous version of the paper: in Microsoft Word if a high quality document is desired one has to check the option "Do not compress images in file" under "Options" - "Advanced". If this is not done Word will use a pre-defined resolution which is typically rather low.

The quality of the images in a pdf document obtained from a Word document can also be improved if when the file is saved as pdf one clicks on "Standard (publishing online and printing)" and before saving the file in the menu "Options" checks the option "ISO 19005-1 compliant (PDF/A)".

The validation tool being precipitation only, it would be preferable if other diagnostics are performed such as vertical profiles versus radio-soundings or any other source of verification.

Given that the BMJ scheme is a convective adjustment scheme where the temperature and humidity profiles are adjusted towards reference thermodynamic profiles we can understand why the reviewer is interested in comparing the WRF vertical profiles of temperature and humidity with those observed by radiosondes.

In *Figures R1 and R2* on the next two pages, we show vertical profiles of temperature and relative humidity for different stations in the western Maritime Continent where we have the largest reduction in precipitation when the BMJ scheme is modified (*Figure 2* of the paper). At all stations, all model profiles are more similar to one another than to the observed. This is somewhat expected as we are comparing the observed vertical profiles with those given by over a grid box by a model run without direct data assimilation. Moreover, at 24km resolution, the model is unable to capture the details of processes important at meso- γ scale. Hence, any good agreement between model and observations at a station would be fortuitous rather than due to the performance of the BMJ scheme itself. We cannot use the observed profiles to evaluate the choice of parameters in the BMJ scheme.

Given that a station sounding taken at a certain time cannot be appropriately compared with the model profile at that time and over that grid box, one may think that we could somehow separately average observations and model profiles over space or time in the hope that model-observation disagreements would be mitigated. Unfortunately, there are only a handful of stations in the Maritime Continent separated by hundreds of kilometres and given the complex topography and land-sea contrasts of the region, averaging the observations or the model profiles over station locations would not be advisable. As for averaging in time, the model is only run for 1 year and given the annual march of the monsoon across

the region, we do not have enough model data to compare with observed seasonally dependent climatological profiles. So validation of the model temperature and humidity profiles remains open and will be attempted in a subsequent paper when we have finished 27 years of model simulation. We are grateful to the reviewer for raising this point.

In any case, taking a step back, the purpose of this paper is not to validate WRF model in totality, but to reduce the rainfall bias inherent in the BMJ scheme, as stated in lines 90 - 93. Therefore, we are comfortable not to include the validation of any variable but rainfall in the present paper.

Furthermore, in line 12 of page 4020, the word "and" should be removed and in line 5 of page 4022, the word "August" should be replaced by September.

We have removed the word "and" and split the sentence. The word "August" was also replaced by "September" in line 5 of page 4022.

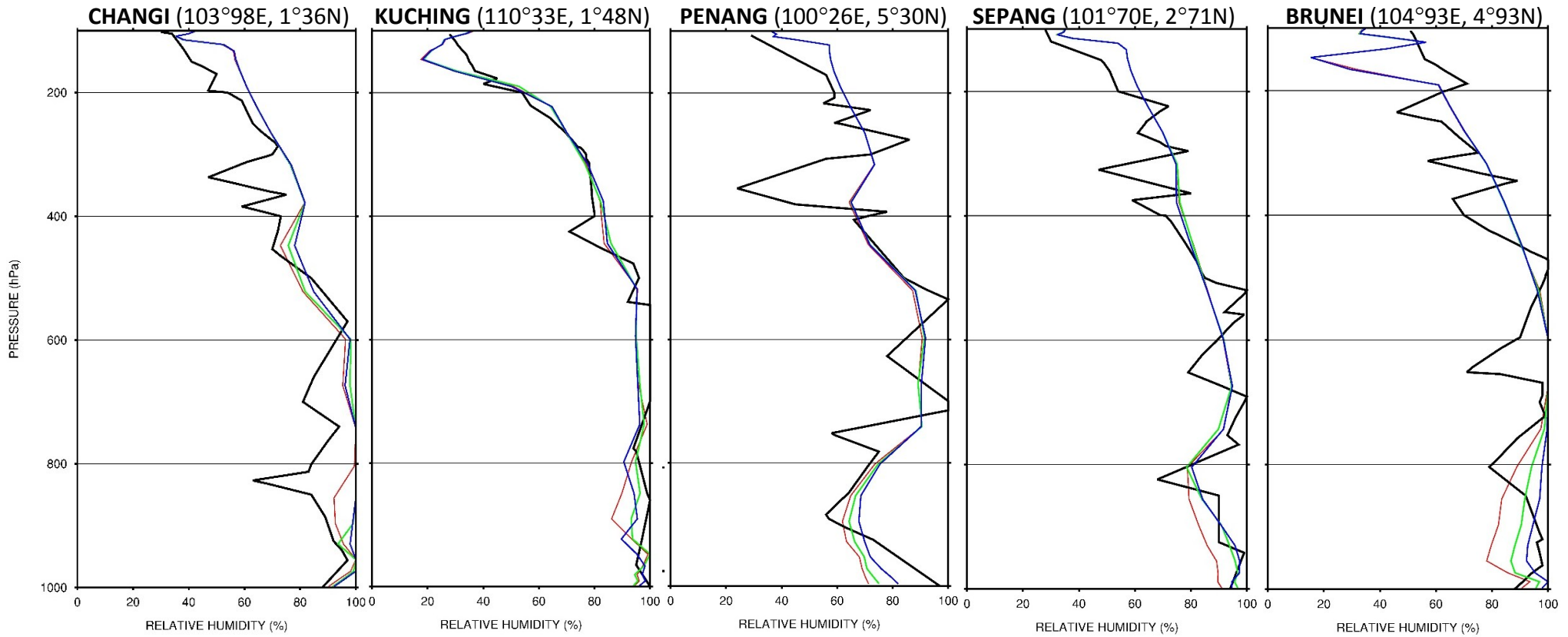


Figure R1: Vertical profiles of relative humidity (units of %) on 3rd March 2008 at 00UTC for the Changi (103°98E, 1°36N), Kuching (110°33E, 1°48N), Penang (100°26E, 5°30N), Sepang (101°70E, 2°71N) and Brunei (104°93E, 4°93N) stations (black curves) using the default WRF-BMJ scheme (red curve) and two experiments with a more moist humidity reference profile ($F_s=0.6$ in green and $F_s=0.3$ in blue). The observed vertical profiles were taken from the University of Wyoming website (<http://weather.uwyo.edu/upperair/sounding.html>).

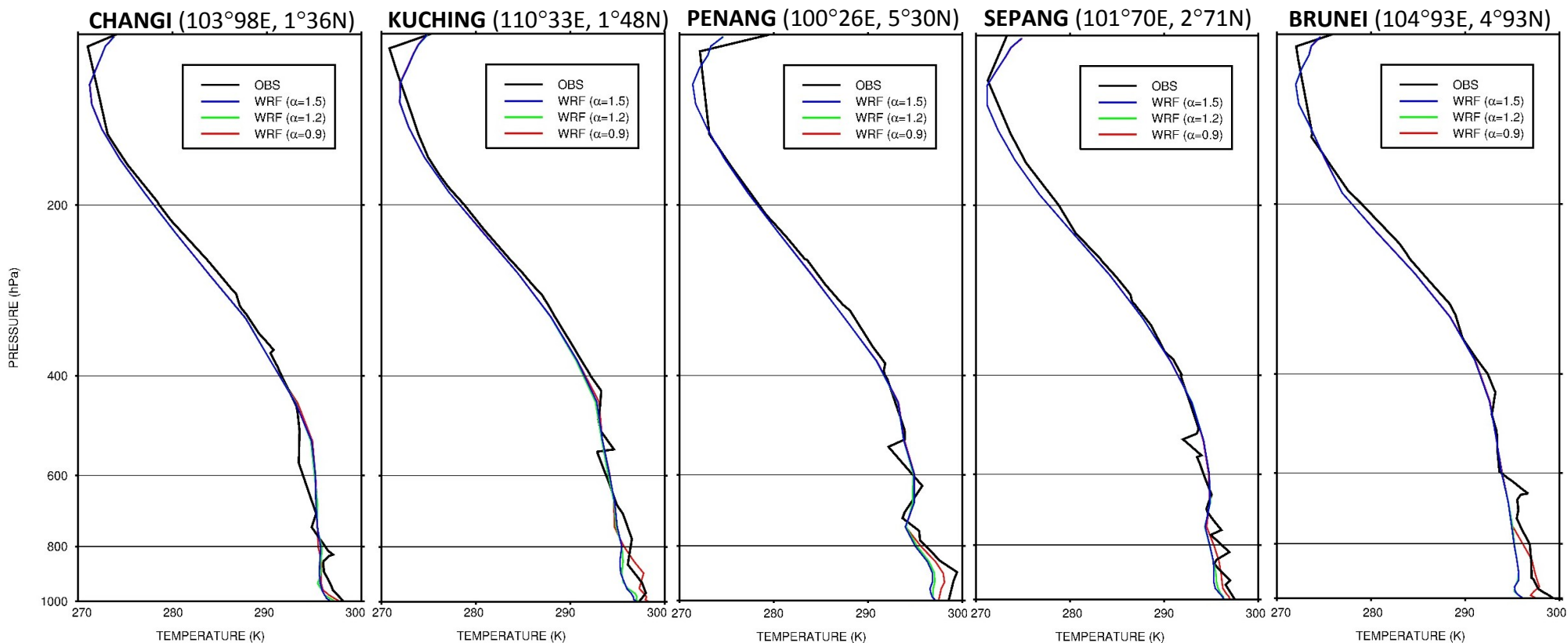


Figure R2: Skew-T Log-P diagrams on 3rd March 2008 at 00UTC for the Changi (103°98E, 1°36N), Kuching (110°33E, 1°48N), Penang (100°26E, 5°30N), Sepang (101°70E, 2°71N) and Brunei (104°93E, 4°93N) stations (black curves) using the default WRF-BMJ scheme (red curve) and two experiments with a warmer temperature reference profile ($\alpha=1.2$ in green and $\alpha=1.5$ in blue). The observed vertical profiles were taken from the University of Wyoming website (<http://weather.uwyo.edu/upperair/sounding.html>).

1
2
3 IMPROVED SIMULATION OF
4 PRECIPITATION IN THE TROPICS
5 USING A MODIFIED BMJ SCHEME IN
6 WRF MODEL

7
8
9
10
11 RICARDO FONSECA

12 Earth Observatory of Singapore, Nanyang Technological University

13 TENGFEI ZHANG

14 School of Physical and Mathematical Sciences, Nanyang Technological University

15 KOH TIEH YONG[†]

16 Earth Observatory of Singapore, Nanyang Technological University

17 School of Physical and Mathematical Sciences, Nanyang Technological University

18
19
20
21
22[†]Corresponding author address: Koh Tieh Yong, Earth Observatory of Singapore, Nanyang Technological University,
N2-01a-15, 50 Nanyang Avenue, Singapore 639798. E-mail: kohty@ntu.edu.sg.

ABSTRACT

23
24
25
26
27
28
29
30
31
32
33
34
35
36
37
38
39
40
41

The successful modelling of the observed precipitation, a very important variable for a wide range of climate applications, continues to be one of the major challenges that climate scientists face today. When the Weather Research and Forecasting (WRF) model is used to dynamically downscale the Climate Forecast System Reanalysis (CFSR) over the Indo-Pacific region, with analysis (grid-point) nudging, it is found that the cumulus scheme used, Betts-Miller-Janjić (BMJ), produces excessive rainfall suggesting that it has to be modified for this region. Experimentation has shown that the cumulus precipitation is not very sensitive to changes in the cloud efficiency but varies greatly in response to modifications of the temperature and humidity reference profiles. A new version of the scheme, ~~denoted~~denominated “modified BMJ” scheme, where the humidity reference profile is more moist, was developed ~~and~~. In tropical belt simulations it was found to give a better estimate of the observed precipitation, as given by the Tropical Rainfall Measuring Mission (TRMM) 3B42 dataset, than the default BMJ scheme for the whole tropics and both monsoon seasons. In fact, in some regions the model even outperforms CFSR. The advantage of modifying the BMJ scheme to produce better rainfall estimates lies in the final dynamical consistency of the rainfall with other dynamical and thermodynamical variables of the atmosphere.

42 1. INTRODUCTION

43

44 One of the major challenges facing regional climate modelers today is the accurate
45 representation of the observed rainfall, in particular in areas with complex topography and
46 land-sea contrasts such as the Maritime Continent (hereafter MC). The MC, which consists of
47 the Malay Peninsula, the Greater and Lesser Sunda Islands and New Guinea, comprises small
48 landmasses with elevated terrain and shallow seas. This is a region of conditional instability
49 that plays an important role in the large-scale atmospheric circulation (Ramage, 1968). When
50 used to simulate the climate of these regions, given their coarse horizontal resolutions, Global
51 Climate Models (hereafter GCMs) fail to capture many of the factors and processes that drive
52 regional and local climate variability, including the regional topography, and so Regional
53 Climate Models (hereafter RCMs), forced by GCMs or re-analysis data, are used instead, to
54 better study the climate of the MC.

55

56 When running a RCM forced with coarse resolution data as lateral boundary conditions,
57 and without any further constraints, the fields in the interior can be quite different from the
58 driving fields (Bowden et al., 2012) meaning that some form of relaxation in the interior,
59 either analysis (Stauffer and Seaman, 1990, 1991) or spectral (Waldron et al., 1996; von
60 Storch et al., 2000) nudging, is required to keep the RCM from diverging too far from the
61 coarse-grid data. In WRF, and in both analysis and spectral nudging, the horizontal winds (u ,
62 v) and the potential temperature perturbation (θ') are relaxed towards a reference state.
63 However, while in the former water vapour mixing ratio (q_v) is also nudged, in the latter the
64 geopotential height perturbation (ϕ) is relaxed instead. The reason why moisture is not
65 nudged in spectral nudging is because of its spatial distribution: it can have pronounced
66 horizontal and especially vertical variations that are likely to be missed out by the coarse

67 resolution re-analyses used to force the RCMs (Miguez-Macho et al., 2005). Given the
68 importance of the water vapour distribution for the simulation of the tropical climate, analysis
69 nudging is employed with the four fields nudged every 6h on a time-scale of ~1h, a typical
70 time-scale used in nudging experiments (Stauffer and Seaman, 1991) and comparable to the
71 critical time-scale needed to properly reproduce the large-scale flow in the tropics (Hoskins et
72 al., 2012). Nudging is only applied above the level of 800hPa, and excluding the Planetary
73 Boundary Layer (hereafter PBL), as this configuration is found to give the best results for this
74 region (Jeff Lo, pers. comm.). In addition, experimentation has shown that the precipitation
75 over Southeast Asia is not very sensitive to the choice of the radiation, PBL, microphysics
76 and land surface schemes but varies greatly with the choice of the cumulus scheme, with the
77 Betts-Miller-Janjić (hereafter BMJ) scheme giving the smallest biases compared to the Kain-
78 Fritsch (Kain and Fritsch, 1990, 1993; Kain, 2004) and Grell-Devenyi (Grell and Devenyi,
79 2002) schemes (Jeff Lo, pers. comm.). However, even when interior nudging is employed,
80 WRF overestimates the observed rainfall, as given by TRMM 3B42 version 6 (Huffman et
81 al., 2007), as seen in *Figure 1*. Here the rainfall rate over Southeast Asia averaged over the
82 2008 boreal summer (June-~~September~~August, JJAS) for TRMM and the WRF experiments
83 with and without analysis nudging is shown. As can be seen, without interior nudging the
84 model produces excessive precipitation in particular in the monsoon regions of southern Asia
85 and to the east of the Philippines as a result of an incorrect representation of the large-scale
86 atmospheric circulation (not shown). When analysis nudging is employed the phase of the
87 WRF precipitation is similar to that of TRMM's but the model continues to overestimate its
88 amplitude. Given that most of the rainfall in these runs is generated by the cumulus scheme,
89 the excessive precipitation produced suggests that the cumulus scheme may have to be
90 modified at least for this region and possibly for the global tropics. The modification of the
91 BMJ scheme to yield better tropical rainfall estimates will be addressed in this paper which

92 will also necessitate a comprehensive discussion of the BMJ scheme as implemented in
93 WRF.

94
95 Despite recent improvements, much work is still needed to successfully develop an accurate
96 representation of cumulus convection in numerical models. There are essentially two widely
97 used types of convection parameterization schemes in weather and climate models: mass-flux
98 or moisture convergence schemes (e.g. Arakawa and Schubert, 1974; Kain and Fritsch, 1990,
99 1993, Kain, 2004; Emanuel, 2001) and adjustment schemes (e.g. Betts, 1986, Betts and
100 Miller, 1986, Janjić, 1994). In the former a one-dimensional cloud model is used to compute
101 the updraft and downdraft mass fluxes and processes such as entrainment and detrainment are
102 also normally considered. In contrast to these increasingly complex parameterizations which
103 can involve detailed models of cloud processes, convective adjustment schemes take an
104 “external” view of convection and simply relax the large-scale environment towards
105 reference thermodynamic profiles. One of such schemes is the Betts-Miller (hereafter BM)
106 scheme that was originally developed by Alan Betts and Martin Miller in the 1980’s and later
107 modified by Zaviša Janjić in the 1990’s to yield the current BMJ scheme. Janjić introduced a
108 parameter called “cloud efficiency” that acts to reduce the precipitation in order to provide a
109 smoother transition to grid-resolved processes.

110
111 The WRF model (Skamarock et al., 2008), a fully compressible and non-hydrostatic
112 model, is used in this work. WRF uses a terrain-following vertical coordinate derived from
113 the hydrostatic pressure and surface pressure and the Arakawa-C grid staggering for
114 horizontal discretization. It is a community model used in a wide variety of applications
115 including idealized simulations (e.g. Steele et al., 2013), hurricane research (e.g. Davis et al.,
116 2008), regional climate research (e.g. Chotamonsak et al., 2011, 2012), weather forecasts
117 (e.g. Done et al., 2004) and coupled atmosphere-ocean modelling (e.g. Samala et al., 2013).

118 Here it is used to investigate the sensitivity of the cumulus precipitation to modifications
119 made to the BMJ scheme and to assess the performance of the “modified BMJ” scheme in
120 tropical belt simulations.

121
122 In Section 2 details about the model setup and methods used are presented. A discussion
123 of the BMJ scheme is given in section 3 while the results obtained in sensitivity experiments
124 are shown in Section 4. In section 5 the focus is on the modified scheme’s performance in
125 tropical belt experiments and in section 6 the main conclusions are presented.

126 2. MODEL, DATASETS AND DIAGNOSTICS

127
128

129 In this study WRF is initialized with CFSR 6-hourly data (Saha et al., 2010; this data was
130 downloaded from the Research Data Archive at the National Center for Atmospheric
131 Research, Computational and Information Systems Laboratory, available online at
132 <http://rda.ucar.edu/datasets/ds093.0/>), horizontal resolution of $0.5^\circ \times 0.5^\circ$, and is run for 1 day
133 (2nd March – 3rd March 2008), 1 month (1st April – 30th April 2008), 6 months (1st April 2008
134 – 30th September 2008) and 10 months (1st June 2008 – 31st March 2009) with a 1-day spin-
135 up in the first set of experiments and a 1-month spin-up time in the last three prior to the
136 stated simulated periods. [The year of 2008 is chosen as according to Ummenhofer et al.](#)
137 [\(2009\) it is a neutral year with respect to both El Niño-Southern Oscillation \(ENSO\) and](#)
138 [Indian Ocean Dipole \(IOD\). By choosing a neutral year, the impact of climatic anomalies is](#)
139 [minimized.](#) The physics parameterizations used include the WRF double-moment five-class
140 microphysics scheme (Lim and Hong, 2010), the Rapid Radiative Transfer Model for Global
141 (RRTMG) models for both shortwave and longwave radiation (Iacono et al., 2008), the
142 Yonsei University planetary boundary layer (Hong et al., 2006) with Monin-Obukhov surface
143 layer parameterization (Monin and Obukhov, 1954), the four-layer Noah land surface model
144 (Chen and Dudhia, 2001) and to parameterize cumulus convection the BMJ scheme (Janjić,
145 1994). In all model runs 6-hourly sea surface temperature (hereafter SST) and monthly values
146 of vegetation fraction and surface albedo are used. WRF is also run with a simple prognostic
147 scheme of the sea surface skin temperature (Zeng and Beljaars, 2005) which takes into
148 account the effects of the sensible, latent and radiative fluxes as well as diffusion and
149 turbulent mixing processes in the vertical. In all model simulations nudging is applied at the
150 lateral boundaries over a nine-gridpoint transition zone while in the top 5 km Rayleigh

151 damping is applied to the wind components and potential temperature on a time-scale of 5 s
152 (Skamarok et al., 2008).

153 The spatial domain on Mercator projection used for the 1-day, 1-month and 4-month
154 diagnostics, shown in *Figure 1*, extends from central Africa to the East Pacific and from
155 about 25°S to 25°N with a horizontal grid spacing of 24km, while for the 10-month
156 experiments a tropical belt extending from about 42°S to 45°N with a horizontal resolution of
157 30km is used. In all model runs 37 vertical levels, more closely spaced in the PBL and in the
158 tropopause region, are used with the model top at 30hPa and the highest un-damped layer at
159 about 70hPa. The time-step used is 1 min and the output is archived every 1h. Analysis
160 nudging is applied to the horizontal winds (u , v), potential temperature perturbation (θ') and
161 water vapour mixing ratio (q_v). These fields are relaxed towards CFSR above 800hPa
162 excluding the PBL on a time-scale of 1h. The WRF rainfall is evaluated against the 3-hourly
163 instantaneous multi-satellite rainfall estimates from TRMM, at a horizontal resolution of
164 $0.25^\circ \times 0.25^\circ$, while all other fields are compared with CFSR. The model outputs on pressure
165 and surface levels are bilinearly interpolated to the CFSR and TRMM grids for evaluation.

166 The model's performance is assessed with different verification diagnostics including the
167 model bias, normalized bias (μ), correlation (ρ), variance similarity (η) and normalized error
168 variance (α_ϵ). The bias is defined as the discrepancy between the model and observations
169 while the normalized bias is given by the bias divided by the standard deviation of the
170 discrepancy between the model and observations (when $|\mu| < 0.3$ the contribution of the bias
171 to the total error is less than ~5% and the biases will not be significant). The correlation is a
172 measure of the phase agreement between the model and observations. The variance similarity
173 is an indication of how the signal amplitude given by the model agrees with that observed and
174 is defined as the ratio of the geometric mean to the arithmetic mean of the modelled and

175 observed variances. The normalized error variance is the variance of the error arising from
176 the disagreements in phase and amplitude, normalized by the combined modelled and
177 observed signal variances. The best model performance corresponds to zero bias and α_ϵ and
178 to ρ and η equal to 1. These diagnostics are defined in equations (A1) – (A5) in *Appendix A*.

179 3. BETTS–MILLER–JANJIĆ (BMJ) CUMULUS SCHEME

180
181

182 The BMJ scheme is an adjustment scheme where the essential principle lies in the
183 relaxation of the temperature and humidity profiles towards reference thermodynamic
184 profiles and precipitation is obtained as a necessary consequence from the conservation of
185 water substance. The equations and factors used in the BMJ scheme, as we found
186 implemented in WRF version 3.3.1, are given in the *Appendix B* which the reader is
187 encouraged to consult. We found two main existing differences in WRF's default
188 implementation from the original formulation as defined in Betts (1986) and Janjić (1994):

189

190 • In the definition of the potential temperature reference profile, (B8), the factor α used is 0.9
191 as opposed to 0.85 as suggested by Betts (1986). A larger α leads to a warmer and more
192 moist reference profile and therefore to a reduction in the precipitation produced by the
193 cumulus scheme;

194

195 • The factor F_S , used in the definition of the humidity reference profile for deep convection,
196 (B12) – (B14), is set to 0.85 while in Janjić (1994), a value of 0.6 is used. The smaller F_S is,
197 the more moist the humidity reference profile will be and, therefore, the smaller the amount
198 of precipitation generated by the scheme.

199

200 In section 4.1 the sensitivity of the precipitation produced by this scheme to α and F_S , as well
201 as to the cloud efficiency E and the convective adjustment time-scale τ , will be investigated.

202

203 4. SENSITIVITY EXPERIMENTS

204

205 4.1 ONE-DAY DIAGNOSTICS

206

207 The aim of these experiments is to investigate the sensitivity of the precipitation
208 produced by the BMJ scheme to changes in some of the parameters used in the scheme. In
209 particular, as the default WRF-BMJ implementation scheme produces excessive rainfall over
210 Southeast Asia, as shown in *Figure 1*, in this section different ways of reducing the cumulus
211 precipitation are explored in order to determine which ones are more efficient.

212 WRF is run from 00UTC on 1st March to 00UTC on 3rd March 2008 with the first day
213 regarded as model spin-up. The results are shown in *Figure 2*. Here the precipitation rate
214 obtained with the default BMJ scheme as implemented in WRF version 3.3.1 (control run) is
215 plotted together with the modification in the rainfall rate for ten experiments with a modified
216 BMJ scheme: in the first experiment the sensitivity to the convective adjustment time-scale τ
217 is explored, in the next three the sensitivity to modifications in some of the parameters used
218 in $F(E)$ (namely c_l , E_l and F_l) is assessed while in the other six experiments the sensitivity
219 to changes in the temperature and humidity reference profiles through modifications in α , F_S
220 and F_R is examined.

221 Given that the precipitation produced by the BMJ scheme is proportional to $F(E)$, (B7), a
222 linear function of the cloud efficiency, E , and inversely proportional to the adjustment time-
223 scale τ , the cumulus rainfall can be reduced by decreasing $F(E)$ and increasing τ . The former
224 can be achieved by lowering the constant c_l used in the definition of the cloud efficiency
225 (B5), reducing F_l or increasing E_l (a higher E_l also means a more moist humidity reference
226 profile and less rainfall). In *Figure 2* the difference in the rainfall rate, with respect to the

227 default WRF-BMJ implementation, when τ is doubled ($\tau=80\text{min}$), c_1 is set to one tenth of its
228 original value ($c_1=0.5$) as well as when $E_1 = 0$ and $F_1 = 0.4$ is shown. The impact of changing
229 these parameters on the cumulus rainfall is negligible. Similar results are obtained to changes
230 in F_2 and E_2 (not shown) which is not surprising as changing F_2 and E_2 is equivalent to
231 changing τ and c_1 , respectively. Hence, the precipitation produced by the BMJ scheme is not
232 very sensitive to changes in $F(E)$ and τ .

233 The rainfall produced by the BMJ scheme can also be modified by changing the reference
234 temperature and/or humidity profiles. The temperature reference profile, defined in (B8),
235 includes a parameter α that when increased will give a warmer (and hence more moist)
236 profile and therefore a reduction in the precipitation. The precipitation can also be decreased
237 by making the humidity reference profile more moist which can be achieved by reducing F_S
238 or F_R , (B12) – (B14). The default value of F_R is 1 and an experiment is performed where it is
239 reduced to 0.9. As shown in *Figure 2(e)*, the BMJ scheme's rainfall is not sensitive to
240 changes in F_R . The default values of F_S and α are 0.85 and 0.9, respectively, and experiments
241 are performed where F_S is reduced to 0.6, the value suggested by Janjić (1994), and 0.3, and
242 α is increased to 1.2 and 1.5. One last run in which both parameters are modified (F_S is
243 reduced to 0.6 and α increased to 1.5) is also performed. As seen in *Figure 2*, the BMJ
244 scheme's rainfall is very sensitive to changes in these two parameters, in particular to α : in
245 fact, when α is set to 1.5 the cumulus scheme produces almost no precipitation (i.e., the
246 convection shuts down).

247 In conclusion, in 1-day runs it is found that the precipitation produced by the BMJ
248 scheme is not sensitive to changes in the cloud efficiency E and $F(E)$ but varies greatly when
249 the humidity and temperature reference profiles are modified. In the next section results from
250 2-month runs performed with a modified BMJ scheme using the new values of F_S and α to

251 further assess how the rainfall produced in those runs compares to that obtained with the
252 default WRF-BMJ implementation and observations (TRMM).

253 4.2 ONE-MONTH DIAGNOSTICS

254

255 The impact on precipitation due to changes in the temperature and humidity reference
256 profiles will now be assessed in 1-month runs. WRF is run from 1st March to 30th April 2008,
257 with the first month being regarded as spin-up. The precipitation rate averaged over April for
258 the experiments with the default BMJ scheme and five modified BMJ schemes is shown in
259 *Figure 3*. In the first two the humidity reference profile is more moist than in the default
260 version of the scheme, with F_S changed to 0.6 and 0.3, but no changes are made to the
261 temperature reference profile; in the following two the temperature reference profile is
262 warmer (and hence the humidity reference profile is more moist) with α set to 1.2 and 1.5;
263 finally, in the last experiment F_S is reduced to 0.6 and α increased to 1.5.

264 When the default WRF-BMJ implementation is used the model overestimates the observed
265 rainfall mainly in the MC, eastern Indian Ocean, central tropical Pacific and in the South
266 Pacific Convergence Zone (hereafter SPCZ). However, the other diagnostics are quite high
267 with typical values of 0.7–0.8 for ρ , 0.8–0.9 for η and 0.2–0.3 for α_ϵ and suggesting that
268 WRF captures well the phase and variance of the observed rainfall resulting in small errors in
269 the rainfall pentad series. As expected, in regions that typically receive very little
270 precipitation, such as the Australian desert and south-eastern parts of the Arabian Peninsula,
271 these diagnostics are rather low scores.

272 Regarding the experiments with a modified BMJ scheme, when F_S is set to 0.6, the value
273 recommended by Janjić (1994), there is a much better agreement with TRMM except over
274 the high terrain (in particular in the islands of New Guinea and Borneo) where the model
275 overestimates the observed rainfall. In these regions the precipitation is mostly produced by
276 the microphysics scheme (not shown). However, there is not much of an improvement in the

277 other three diagnostics as they are already good. When a smaller value of F_S is used,
278 corresponding to an even more moist humidity reference profile, there is a significant
279 reduction in the precipitation over the whole domain, with the model now producing less
280 rainfall than TRMM, with a slight worsening of the other diagnostics in particular of η and α_ϵ
281 and over the eastern Indian Ocean, MC and West Pacific. As found in the previous section,
282 the sensitivity of the cumulus precipitation to changes in the temperature reference profile is
283 even larger: when α is increased to 1.2 the scheme produces very little rainfall and a further
284 increase to 1.5 leads to precipitation being confined mainly to the ITCZ, SPCZ and the high
285 terrain, indicating that the convection nearly shuts down. For these experiments there is a
286 significant deterioration of the other three diagnostics in particular of η and α_ϵ . When α is
287 increased to 1.5 and F_S decreased to 0.6 the model performance is similar to that obtained
288 when only α is set to 1.5 but drier than when only F_S is set to 0.6 stressing the fact that α is
289 the limiting factor and not F_S .

290 In conclusion, in two-month experiments it is found that, out of the different options
291 considered, the best agreement with TRMM is obtained when F_S is set to 0.6, the value
292 recommended by Janjić (1994), corresponding to a more moist humidity reference profile
293 while keeping α at its default value of 0.9. This new implementation of the BMJ scheme,
294 hereafter called “modified” BMJ, will now be tested in 6-month runs.

295

296

297

298 4.3 FOUR-MONTH DIAGNOSTICS

299

300 In 1-month runs it is found that the best agreement in the rainfall rate between WRF and
301 TRMM is obtained when F_S is set to 0.6, corresponding to a more moist humidity reference
302 profile. In this section the performance of this modified BMJ scheme will be tested in 6-
303 months runs initialised on 1st April with a focus on the boreal summer season, June to
304 September. In addition, this experiment is also repeated with no interior nudging and relaxing
305 the water vapour mixing ratio, horizontal winds and potential temperature perturbation
306 separately towards CFSR. The results are shown in *Figure 4*.

307 As seen in *Figure 4*, when the modified BMJ scheme is used there is a significant
308 improvement in the representation of the observed rainfall, as given by TRMM, compared to
309 that obtained with the default WRF-BMJ implementation: the positive biases with the default
310 BMJ scheme over the MC and Southeast Asia are corrected when the modified BMJ scheme
311 is used. In fact, with the modified BMJ scheme the model bias is only significant mainly over
312 the high terrain, where most of the rainfall is actually produced by the microphysics scheme.
313 There is an exception around Sri Lanka, however, where there is little precipitation in TRMM
314 but WRF produces a considerable amount of rainfall and therefore the biases will be
315 significant here. There is also some improvement in the other verification diagnostics (not
316 shown).

317 In all WRF experiments discussed so far analysis nudging was employed. However, it is of
318 interest to assess the modified BMJ scheme's performance when no interior nudging is used.
319 The fourth and fifth rows of *Figure 4* show the precipitation obtained with the default and
320 modified BMJ schemes but with no interior nudging applied and they convey a very different
321 picture: in this case there is almost no improvement in the simulation of the observed

322 precipitation when the modified BMJ scheme is used as the decrease in the cumulus rainfall
323 is offset by an increase in the microphysics precipitation. This is an important result that
324 suggests any change made to the BMJ scheme will be fruitless without interior (analysis)
325 nudging. In the default configuration, as stated in section 2, the horizontal winds (u,v),
326 potential temperature perturbation (θ) and water vapour mixing ratio (q_v) are relaxed towards
327 CFSR. Three additional experiments are performed with the modified BMJ scheme where
328 these variables are nudged separately. As shown in *Figure 4*, the crucial variable that has to
329 be relaxed is the water vapour mixing ratio, q_v : in fact, when only this field is nudged the
330 precipitation produced by the model is very similar to that obtained when all four fields are
331 relaxed toward CFSR with similar contributions to rainfall from the cumulus and
332 microphysics schemes. If analysis nudging is only applied to the temperature or horizontal
333 winds there are much larger biases. When only the former is nudged there is excessive
334 precipitation from microphysics off the east coast of India and the Bay of Bengal, as in the
335 experiment with no interior nudging, because of an incorrect representation of the large-scale
336 circulation, as well as to the north-east of New Guinea with the ITCZ in the Pacific displaced
337 southwards. When only the horizontal winds are nudged there is excessive precipitation in a
338 region aligned in the southwest-northeast direction to the west of Sumatra as well as along
339 the ITCZ in the Pacific as a result of excessive moisture in those regions (not shown). In
340 these two experiments, and as opposed to the ones where only q_v or all four fields are relaxed,
341 the microphysics rainfall gives a contribution as large as, or even larger than, the cumulus
342 rainfall to the total precipitation. It can be concluded that it is crucial to properly represent the
343 water vapour mixing ratio in the tropics in order to simulate the observed precipitation. It is
344 also important to stress that here the focus has just been on the precipitation and when only
345 one of the referred fields is nudged separately there are noticeable errors in others and hence

346 all four fields have to be nudged in order for the model to correctly simulate the atmospheric
347 circulation over Southeast Asia (Bowden et al., 2013).

348 5. TROPICAL BELT EXPERIMENTS

349

350 The performance of the modified BMJ will now be assessed for the whole tropics and
351 for 11-months initialised on 1st May 2008 with the first month as spin-up. We focus on the
352 boreal summer monsoon season, JJAS 2008, and winter monsoon season, December to
353 February (hereafter DJFM) straddling 2008 and 2009. The results are shown in *Figure 5*.

354 In the boreal summer, the precipitation produced by WRF in Southeast Asia in the tropical
355 belt experiments is similar to that obtained in the smaller domain runs performed at 24km
356 horizontal resolution shown in *Figure 4*. With the default WRF-BMJ implementation, WRF
357 produces excessive precipitation over most of Southeast Asia and the East Equatorial Pacific
358 with rainfall biases that are also significant over high terrain, in particular over the East
359 African Highlands, the Himalayas, the Arakan Mountains in western Myanmar and the
360 Andes. When the modified BMJ scheme is employed, there is a significant improvement with
361 the biases being now restricted to the high terrain as well as around Sri Lanka (as explained
362 before in section 4). The change in the other verification diagnostics (ρ , η and α_ϵ) is small as
363 they are already relatively good.

364 As also shown in *Figure 5*, similar results are obtained for the boreal winter season: with the
365 default WRF-BMJ implementation the model overestimates the precipitation in the MC and
366 along the SPCZ, but these biases are largely corrected when the modified BMJ scheme is
367 used. However, over land areas such as the Amazon and south-central Africa, and despite
368 some improvement, the model continues to overestimate the observed precipitation. This is
369 because the convective clouds produced by the BMJ scheme are radiatively transparent so
370 that surface temperature remains too warm during rainfall, an issue that will be addressed in a
371 subsequent paper. As was the case for the summer season, very little improvement is seen in

372 ρ , η and α_ϵ when the modified BMJ scheme is used with typical correlations of 0.6–0.8,
373 variance similarity close to 1 and normalized error variances of 0.3–0.4 over most of the
374 domain except in regions with light and irregular amounts of precipitation, such as eastern
375 side of sub-tropical Pacific and Atlantic Oceans and deserts in northern and southern Africa
376 and Arabian Peninsula, Tibetan plateau, Australia and South America. The southern Amazon
377 basin experiences dry season in boreal summer and so η and α_ϵ indicate bad model
378 performance in that season

379 The improvement in the representation of the observed precipitation when the modified BMJ
380 scheme is used is not just confined to Southeast Asia in the boreal summer season, but takes
381 place across the whole tropics and in both monsoon seasons. It is important to note that not
382 all biases are corrected, in particular over high terrain where most rainfall is produced by the
383 microphysics scheme. In these regions WRF is known to overestimate the rainfall, as
384 discussed in Teo et al. (2011), and an accurate simulation of the precipitation requires higher
385 horizontal resolution to properly resolve the orography which we cannot afford
386 computationally in this larger domain.

387 6. CONCLUSIONS

388

389 The accurate modelling of precipitation, in particular over complex topography and
390 regions with strong land-sea contrasts such as the MC, continues to be one of the major
391 challenges that atmospheric scientists face today. In this study the BMJ scheme, a convective
392 adjustment scheme where temperature and humidity are relaxed towards reference profiles, as
393 implemented in WRF version 3.3.1, is modified so that the precipitation produced by the
394 model is in better agreement with that observed as given by TRMM.

395 In 1-day runs the sensitivity of the precipitation to changes in some of the parameters
396 used in the cumulus scheme is investigated. It is found that the rainfall is not sensitive to: τ ,
397 the convective time-scale; $F(E)$, a linear function of the cloud efficiency; F_R , the upper limit
398 to dehumidification by rain formation. The same is not the case when the temperature and
399 humidity reference profiles are modified by changes in the parameters α and F_S . When the
400 temperature reference profile is warmer (corresponding to a larger α) and/or the humidity
401 reference profile is more moist (corresponding to a larger α or a smaller F_S) there is a
402 decrease in the convective rainfall and vice-versa.

403 In 1-month experiments it is found that, out of the different values of α and F_S considered, the
404 best agreement of the model's precipitation with the one given by TRMM is obtained with a
405 more moist humidity reference profile with the parameter F_S set to 0.6, the value suggested
406 by Janjić (1994). This new value is adopted as the modification to the BMJ scheme in
407 subsequent work.

408 From the 4-month diagnostics during JJAS 2008, the rainfall generated by WRF with the
409 modified BMJ scheme is found to be in close agreement with that of TRMM. In fact, the
410 biases are now restricted to high terrain where most of the rainfall is generated by the

411 microphysics scheme. In these experiments analysis nudging is applied in the interior of the
412 domain. Experimentation showed that with no interior nudging the decrease in the rainfall
413 given by the cumulus scheme is mostly offset by an increase in the microphysics rainfall.
414 This result shows that any changes made to the BMJ scheme will only have an impact in the
415 precipitation if some form of nudging in the interior of the model domain is applied. It is also
416 found that the rainfall obtained when only specific humidity is nudged is similar to that
417 obtained when wind and perturbation potential temperature are additionally nudged stressing
418 the importance of modelling well the water vapour distribution in the tropics to successfully
419 produce the observed rainfall.

420 The performance of the modified BMJ scheme is further assessed in tropical belt
421 experiments with the model run from 1st May 2008 to 31th March 2009 with a focus on the
422 boreal summer monsoon, JJAS, and boreal winter monsoon, DJFM. It is found that for both
423 seasons and for the whole tropics, with the modified BMJ scheme the model gives a better
424 estimate of the observed precipitation than the default WRF-BMJ implementation. However,
425 WRF continues to overestimate the observed rainfall over high terrain where a higher
426 horizontal resolution is needed to properly resolve the orography. Although there is a
427 significant reduction in the bias with the modified BMJ scheme, the other three verification
428 diagnostics considered (ρ , η and α_ϵ) do not show much of an improvement as they are
429 already good.

430 To conclude, the modified BMJ scheme gives a better representation of the observed
431 rainfall for the whole tropics in both winter and summer seasons, and will be of a great value
432 to the research community working on tropical dynamics. Progress has also been made in
433 understanding how the BMJ scheme, as implemented in WRF, interacts with other physics
434 schemes, in particular with the microphysics scheme.

435 **APPENDIX A: VERIFICATION DIAGNOSTICS** ~~USED TO ASSESS~~
436 ~~THE WRF MODEL'S PERFORMANCE~~

437
438
$$BIAS = \langle \mathbf{D} \rangle = \langle \mathbf{F} \rangle - \langle \mathbf{O} \rangle \quad (A1)$$

439
440
$$\mu = \frac{\langle \mathbf{D} \rangle}{\sigma_D} \quad (A2)$$

441
442
$$\rho = \frac{1}{\sigma_O \sigma_F} \langle (\mathbf{F} - \langle \mathbf{F} \rangle) \cdot (\mathbf{O} - \langle \mathbf{O} \rangle) \rangle, \quad -1 \leq \rho \leq 1 \quad (A3)$$

443
444
$$\eta = \frac{\sigma_O \sigma_F}{\frac{1}{2}(\sigma_O^2 + \sigma_F^2)}, \quad 0 \leq \eta \leq 1 \quad (A4)$$

445
446
$$\alpha_\epsilon = 1 - \rho\eta = \frac{\sigma_D^2}{\sigma_O^2 + \sigma_F^2}, \quad 0 \leq \alpha \leq 2 \quad (A5)$$

447
448 In the equations above \mathbf{D} is the discrepancy between the model forecast \mathbf{F} and the
449 observations \mathbf{O} ; σ_X is the standard deviation of X ; μ is the normalized bias; ρ is the
450 correlation coefficient; η is the variance similarity; α_ϵ is the normalized error variance.

451 More information about these diagnostics can be found in Koh et al. (2012).

454 APPENDIX B: BMJ EQUATIONS FOR DEEP CONVECTION IN WRF

455 The equations shown in this section are the ones used in the BMJ scheme in WRF Version
456 3.3.1 and are based on Betts (1986) and Janjić (1994).

457 In this cumulus scheme as explained in Betts (1986), the model first assesses whether there is
458 Convective Available Potential Energy (CAPE) present and whether the cloud is sufficiently
459 thick (i.e., $L_B - L_T > 2$ or $p_B - p_T > 10hPa$ where L_B and L_T are the cloud-base and cloud-
460 top model levels and p_B and p_T the correspondent pressure levels; L_B is defined as the model
461 level just above the Lifting Condensation Level (LCL) and has to be at least 25hPa above the
462 surface whereas L_T is defined as the level at which CAPE is maximum (i.e., level of neutral
463 buoyancy, LNB) for the air parcel with the maximum equivalent potential temperature θ_E in
464 the depth interval $[PSFC, PSFC \times 0.6]$ where $PSFC$ is the surface pressure. If that is not the
465 case there will be no convection and the scheme will abort. If all those conditions are met, the
466 cloud depth is compared to a minimum depth given by

$$D_{min} = 200hPa \left(\frac{PSFC}{1013hPa} \right) \quad (B1)$$

467
468 If the cloud depth is smaller than D_{min} , shallow convection is triggered; otherwise, deep
469 convection is considered. In both shallow and deep convection (Betts, 1986), temperature and
470 humidity fields are adjusted as follows

$$\begin{aligned} \Delta T_{BM} &= T_{REF} - T \\ \Delta q_{BM} &= q_{REF} - q \end{aligned} \quad (B2)$$

471
472 where ΔT_{BM} and Δq_{BM} are the Betts' adjustment of temperature T and specific humidity q in a
473 model layer. Thus, the problem is reduced to defining the reference temperature and specific

474 humidity reference profiles T_{ref} and q_{ref} for shallow and deep convection. In the BMJ
 475 scheme rainfall is only produced by deep convection which is the topic of this appendix.

476

477 RAINFALL

478 The BM scheme conserves enthalpy meaning that

$$\sum_{p_T}^{p_B} (c_P \Delta T_{BM} + L_{WV} \Delta q_{BM}) \Delta p_L = 0 \quad (B3)$$

479 where c_P is the specific heat at constant pressure for dry air assumed to be constant; L_{WV} is
 480 the latent heat of vaporisation for water vapour; Δp_L is the thickness of the model layer
 481 bounded by the model level indices L and $L + 1$ in pressure coordinate. The total mass of
 482 water substance is conserved and hence in the original BM scheme (Betts, 1986) the rainfall
 483 is given by

$$\Delta P_{BM} = \frac{1}{g \rho_w} \sum \Delta q_{BM} \Delta p_L \quad (B4)$$

485

486

487 where ρ_w is the density of liquid water; g is the acceleration of free fall.

488 In Janjić (1994), a parameter called cloud efficiency, E , is introduced and is defined as

$$E = c_1 \frac{\bar{T} \Delta S}{c_P \sum \Delta T_{BM} \Delta p_L} \quad (B5)$$

489

490 with

$$\bar{T} = \frac{\sum T_m \Delta p_L}{p_{bottom} - p_{top}}$$

$$\Delta S = \sum \left(\frac{c_P \Delta T_{BM} + L_{WV} \Delta q_{BM}}{T_m} \right) \Delta p_L$$

$$T_m = T + \frac{\Delta T_{BM}}{2}$$

491

492 where \bar{T} is the weighted mean temperature of the cloudy air column; ΔS is the entropy change
 493 per unit area for the cloudy air column multiplied by g ; T_m is the mean temperature over the
 494 time-step; c_1 is a non-dimensional constant estimated experimentally and set to 5. All
 495 summation symbols refer to summing over all cloudy layers [L_B, L_T].

496 The denominator of (B5) is proportional to the single time-step rainfall from a model layer in
 497 the original BM scheme, (B4), and hence the cloud efficiency reduces when there is a
 498 propensity for heavy rain, partly correcting the tendency to over-predict intense rainfall in the
 499 original BM scheme.

500

501 In the default WRF-BMJ implementation, the precipitation, ΔP , and the adjustments in
 502 temperature and humidity, ΔT and Δq , over one cumulus time-step Δt are given by

$$\begin{cases} \Delta P = \Delta P_{BM} F(E) \Delta t / \tau \\ \Delta T = \Delta T_{BM} F(E) \Delta t / \tau \\ \Delta q = \Delta q_{BM} F(E) \Delta t / \tau \end{cases} \quad (B6)$$

503

504 where $F(E)$ is a linear function of the cloud efficiency given by

$$F(E) = \left(1 - \frac{\Delta S_{min}}{\Delta S} \right) \left[F_1 + (F_2 - F_1) \left(\frac{E' - E_1}{E_2 - E_1} \right) \right] \quad (B7)$$

505

506 with E' constrained to be in the range [E_1, E_2]:

$$E' = \begin{cases} E_1 & \text{if } E \leq E_1 \\ E & \text{if } E_1 \leq E \leq E_2 \\ E_2 & \text{if } E \geq E_2 \end{cases}$$

507

508 The constant $F_1 = 0.7$ is determined experimentally and $F_2 = 1$ for the chosen value of
 509 τ while $E_1 = 0.2$ is determined empirically in Janjić (1994) and $E_2 = 1$ for the chosen value
 510 of c_1 . It is important to note that in Janjić (1994), $F(E)$ does not depend on the entropy
 511 change unlike the implementation we found in WRF version 3.3.1. In (B6) τ is the convective
 512 adjustment time-scale set to 40 min (Betts, 1986).

513 If the change in entropy is small (or even negative), i.e. $\Delta S < \Delta S_{min} = 10^{-4} JK^{-1}m^{-1}s^{-2}$,
 514 or very little (perhaps even negative) rainfall is obtained, i.e. $\sum \Delta T \Delta p_L \leq$
 515 $10^{-7} Kkgm^{-1}s^{-2}$, shallow convection is triggered; otherwise, the BMJ scheme proceeds
 516 with deep convection. The reader is referred to Janjić (1994) for the documentation on
 517 shallow convection which we are not concerned with in this work.

518

519 **REFERENCE PROFILES FOR DEEP CONVECTION**

520 The first-guess potential temperature reference profile θ_{REF}^f for deep convection used in the
 521 BMJ scheme is assumed to have a vertical gradient that is a fixed fraction α of the vertical
 522 gradient of saturated equivalent potential temperature θ_{ES} following a moist virtual adiabat
 523 (i.e. isopleth of virtual equivalent potential temperature) from the cloud base up to the
 524 freezing level. Above the freezing level, θ_{REF}^f slowly approaches and reaches the
 525 environmental θ_{ES} at the cloud top. Thus, θ_{REF} given is prescribed by

$$\theta_{REF}^f(p_B) = \theta(p_0, T_0)$$

526

$$\left\{ \begin{array}{l} p_M \leq p_L < p_B: \quad \theta_{REF}^f(p_L) = \theta_{REF}^f(p_{L-1}) + \alpha [\theta_{ES}(p_L) - \theta_{ES}(p_{L-1})] \\ p_T \leq p_L < p_M: \quad \theta_{REF}^f(p_L) = \theta_{ES}(p_L) - \frac{p_L - p_T}{p_M - p_T} \{ \theta_{ES}(p_M) - \theta_{REF}^f(p_M) \} \end{array} \right. \quad (B8)$$

527
528 where p_M denotes the pressure at the freezing model level, p_L denotes the pressure at any
529 model level in the cloudy air column (such that L increases upwards from p_B to p_T) and
530 p_0 and T_0 the pressure and temperature at the level from which the air parcel is lifted. In the
531 first equation the constant α , according to Betts (1986), is equal to 0.85 but in the default
532 WRF implementation it is set to 0.9, corresponding to a steeper $d\theta_{REF}/dp$ or a statically
533 more stable profile. This choice of 0.9 for α was made when the scheme was tuned to the
534 model over the North American region (Zaviša, pers. comm.).

535 The corresponding first-guess reference temperature profile is

$$T_{REF}^f(p_L) = \theta_{REF}^f(p_L) \Pi(p_L) \quad (B9)$$

536
537 with

$$\Pi(p_L) = \left(\frac{10^5 \text{ Pa}}{p_L} \right)^{-R/c_p}$$

538
539 where $\Pi(p_L)$ is the Exner's function (divided by c_p) for pressure p_L and R is the specific gas
540 constant for dry air.

541 At pressure p_L equal or lower than 200hPa, the humidity field is not adjusted by the BMJ
542 scheme. At pressure p_L larger than 200hPa in the convecting column, the first-guess reference
543 specific humidity, $q_{REF}^f(p_L)$, is prescribed by the lifting condensation level, $p_L + \wp(p_L)$, of
544 an air parcel with $\theta_{REF}(p_L)$ and $q_{REF}^f(p_L)$ at pressure p_L ,

$$\begin{cases} q_{REF}(p_L) = q(p_L) & \text{if } p_L \leq p_{200} \\ q_{REF}^f(p_L) = q^*(\theta_{REF}^f(p_L), p_L + \wp(p_L)) & \text{if } p_L > p_{200} \end{cases} \quad (B10)$$

545

546 where p_{200} is the pressure of a model level just smaller or equal to 200hPa. With the help of
 547 Tetens' formula (Tetens, 1930), the saturated specific humidity q^* is given by

$$q^*(\theta_{REF}^f(p_L), p_L + \wp(p_L)) = \left(\frac{379.90516 \text{ Pa}}{p_L + \wp(p_L)} \right) EXP \left\{ 17.2693882 \left(\frac{\theta_{REF}^f(p_L) - \frac{273.16 \text{ K}}{\Pi(p_L + \wp(p_L))}}{\theta_{REF}^f(p_L) - \frac{35.86 \text{ K}}{\Pi(p_L + \wp(p_L))}} \right) \right\} \quad (B11)$$

548

549 The more negative $\wp(p_L)$ is, the drier the reference profile is at pressure level p_L . $\wp(p_L)$ is
 550 piecewise linearly interpolated between the values at the cloud bottom, \wp_B , freezing level,
 551 \wp_M , and cloud top, \wp_T , which are in turn parameterized as linear functions of cloud
 552 efficiency E as follows:

$$\wp_B = (-3875 \text{ Pa}) \left[F_S + (F_R - F_S) \left(\frac{E' - E_1}{E_2 - E_1} \right) \right] \quad (B12)$$

$$\wp_M = (-5875 \text{ Pa}) \left[F_S + (F_R - F_S) \left(\frac{E' - E_1}{E_2 - E_1} \right) \right] \quad (B13)$$

$$\wp_T = (-1875 \text{ Pa}) \left[F_S + (F_R - F_S) \left(\frac{E' - E_1}{E_2 - E_1} \right) \right] \quad (B14)$$

553

554 The constants in Pa above were determined by Janjić (1994) and are not varied in this work.
 555

556 In the WRF version 3.3.1 implementation, the parameter F_R is set to 1 while F_S is set to 0.85,
 557 an empirically determined value over continental USA (Zaviša, pers. comm.), while in the
 558 Janjić (1994) $F_S = 0.6$. Evidently, with a higher value of F_S , the formulation yields more
 559 negative $\wp(p_L)$ and a drier reference humidity profile for each cloud efficiency, $E < E_2$.

560

561

562 **ACKNOWLEDGMENTS**

563 We are thankful to Bob Dattore (UCAR) for his help in downloading CFSR data through the
564 CISL RDA website. This work comprises Earth Observatory of Singapore contribution no.
565 85. It is supported by the National Research Foundation Singapore and the Singapore
566 Ministry of Education under the Research Centres of Excellence initiative. Special thanks are
567 owed to Chee Kiat Teo, Yudha Djamil, Shunya Koseki, Jagabandhu Panda, Fang Wan, Ken
568 Tay and Xianxiang Li who generously made many constructive suggestions.

569

570

571 **REFERENCES**

572

573 Arakawa, A. and Schubert, W. H.: Interaction of a cumulus cloud ensemble with the large-scale
574 environment, Part I. *J. Atmos. Sci.*, 31, 674-701, 1974

575

576 Betts, A. K.: A new convective adjustment scheme. Part I: Observational and theoretical basis. Non-
577 precipitating cumulus convection and its parameterization, *Q. J. R. Meteorol. Soc.*, 112, 677-691,
578 1986.

579

580 Betts, A. K. and Miller, M. J.: A new convective adjustment scheme. Part II: Single column tests using
581 GATE wave, BOMEX, ATEX and arctic air-mass data sets, *Q. J. R. Meteorol. Soc.*, 112, 693-709,
582 1986.

583

584 Bowden, J. H., Otte, T. L., Nolte, C. G. and Otte, M. J.: Examining Interior Analysis nudging
585 Techniques Using Two-Way Nesting in the WRF Model for Regional Climate Modeling, *J. Climate*
586 25, 2805-2823, 2012.

587

588 Bowden, J. H., Nolte, C. G. and Otte, T. L.: Simulating the impact of the large-scale circulation on the
589 2-m temperature and precipitation climatology, *Clim. Dyn.* 40, 1903-1920, 2013.

590

591 Chen, F. and Dudhia, J.: Coupling an advanced land surface–hydrology model with the Penn State–
592 NCAR MM5 modeling system. Part I: Model implementation and sensitivity, *Mon. Wea. Rev.*, 129,
593 569-585, 2001.

594

595 Chotamonsak, C., Salathe E. P., Kreasuwan, K. and Chantara, S.: Evaluation of Precipitation
596 Simulations over Thailand using a WRF Regional Climate Model, *Chiang Mai J. Sci.*, 39, 623-638,
597 2012.

598

599 Chotamonsak, C., Salathe, E. P., Kreasuwan, K., Chantara, S. and Siriwitayakorn, K.: Projected
600 climate change over Southeast Asia using a WRF regional climate model, *Atmos. Sci. Lett.*, 12, 213-
601 219, 2011.

602

603 Davis, C., Wang, W., Chen, S. S., Chen, Y., Corbosiero, K., DeMaria, M., Dudhia, J., Holland, G.,
604 Klemp, J., Michalakes, J., Reeves, H., Rotunno, R., Snyder, C. and Xiao, Q.: Prediction of
605 Landfalling Hurricanes with the Advanced Hurricane WRF Model, *Mon. Wea. Rev.*, 136, 1990-2005,
606 2008.

607

608 Done, J., Davis, C. A. and Weisman, M.: The next generation of NWP: explicit forecasts of
609 convection using the weather research and forecasting (WRF) model, *Atmosph. Sci. Lett.*, 5, 100-117,
610 2004.

611

612 Emanuel, K. A.: A scheme for representing cumulus convection in large-scale models, *J. Atmos. Sci.*
613 48, 2313-2335, 2001.

614

615 Grell, G. A. and Dévényi, D.: A generalized approach to parameterizing convection combining
616 ensemble and data assimilation techniques, *Geophys. Res. Lett.*, 29(14), 2002.

617

618 Hong, S.-Y., Noh, Y. and Dudhia, J.: A New Vertical Diffusion Package with an Explicit Treatment of
619 Entrainment Processes, *Mon. Wea. Rev.*, 134, 2318–2341, 2006

620

621 Hoskins, B. J., Fonseca, R. M., Blackburn, M. and Jung, T.: Relaxing the Tropics to an ‘observed’
622 state: analysis using a simple baroclinic model, *Quart. J. Roy. Meteor. Soc.*, 138, 1618-1626, 2012.

623

624 Huffman, G. J., Alder, R. F., Bolvin, D. T., Gu, G., Nelkin, E. J., Bowman, K. P., Hong, Y., Stocker,
625 E. F. and Wolff, D. B.: The TRMM multisatellite image precipitation analysis (TMPA). Quasi-global,

626 multi-year, combined-sensor precipitation estimates at fine scales, *J. Hydrometeor.*, 8, 38-55, 2007.
627

628 Iacono, M. J., Delamere, J. S., Mlawer, E. J., Shephard, M. W., Clough, S. A. and Collins, W. D.:
629 Radiative forcing by long-lived greenhouse gases: Calculations with the AER radiative transfer
630 models, *J. Geophys. Res.*, 113, D13103, doi:10.1029/2008JD009944, 2008.
631

632 Janjić, Z. I.: The step-mountain eta coordinate model: further developments of the convection, viscous
633 sublayer and turbulence closure schemes, *Mon. Wea. Rev.*, 122, 927-945, 1994.
634

635 Kain, J. S.: The Kain-Fritsch convection parameterization: an update, *J. Appl. Meteorol.*, 43, 170-181,
636 2004.
637

638 Kain, J. S. and Fritsch, J. M.: A one-dimensional entraining/detraining plume model and its
639 application in convective parameterization, *J. Atmos. Sci.*, 47, 2784-2802, 1990.
640

641 Kain, J. S. and Fritsch, J. M.: Convective parameterization for mesoscale models: the Kain-Fritsch
642 scheme. *The Representation of Cumulus Convection in Numerical Models*, *Meteorol. Monogr.*, 24,
643 165-170, Amer. Meteor. Soc., 1993.
644

645 Koh, T.-Y., Wang, S. and Bhatt, B. C.: A diagnostic suite to assess NWP performance, *J. Geophys.*
646 *Res.*, 117, D13109, doi:10.1029/2011JD017103, 2012.
647

648 Lim, K., Hong, S.: Development of an effective double-moment cloud microphysics scheme with
649 prognostic cloud condensation nuclei (CCN) for weather and climate models, *Mon. Wea. Rev.*, 138,
650 1587–1612, 2010.
651

652 Miguez-Macho, G., Stenchikov, G. L. and Robock, A.: Regional climate simulations over North-
653 America: interaction of local processes with improved large-scale flow, *J. Climate.*, 18, 1227-1246,

654 2005.

655

656 Monin, A. S. and Obukhov, A. M.: Basic laws of turbulent mixing in the ground layer of the
657 atmosphere, *Trans. Geophys. Inst. Akad. Nauk USSR*, 151, 163-187, 1954.

658

659 Ramage, C. S.: The role of a tropical “maritime continent” in the atmospheric circulation, *Mon. Wea.*
660 *Rev.*, 96, 365–370, 1968.

661

662 Saha, S., Moorthi, S., Pan, H.-L., Wu, X., Wang, J., Nadiga, S., Tripp, P., Kistler, R., Woollen, J.,
663 Behringer, D., Liu, H., Stokes, D., Grumbine, R., Gayno, G., Wang, J., Hou, Y.-T., Chuang, H.-Y.,
664 Juang, H.-M. H., Sela, J., Iredell, M., Treadon, R., Kleist, D., Delst, P. V., Keyser, D., Derber, J., Ek,
665 M., Meng, J., Wei, H., Yang, R., Lord, S., Dool, H., Kumar, A., Wang, W., Long, C., Chelliah, M.,
666 Xue, Y., Huang, B., Schemm, J.-K., Ebisuzaki, W., Lin, R., Xie, P., Chen, M., Zhou, S., Huggins, W.,
667 Zou, C.-Z., Liu, Q., Chen, Y., Han, Y., Cucurull, L., Reynolds, R. W., Rutledge, G. and Goldberg, M.:
668 The NCEP Climate Forecast System Reanalysis, *Bull. Amer. Meteor. Soc.*, 91, 1015-1057, 2010.

669

670 Samala, B. K., Nagaraju, C., Banerjee, S., Kaginalkar, S.A. and Dalvi, M.: Study of the Indian
671 summer monsoon using WRF–ROMS regional coupled model simulations, *Atmosph. Sci. Lett.*, 14,
672 20–27, doi:10.1002/asl2.409, 2013.

673

674 Skamarock, W. C., Klemp, J. B., Dudhia, J., Gill, D. O., Barker, D. M., Duda, M. G., Huang, X.-Y.,
675 Wang, W. and Powers, J. G.: A description of the Advanced Research WRF version 3, NCAR tech.
676 Note TN-4175_STR, 113pp, 2008.

677

678 Stauffer, D. R. and Seaman, N. L.: Use of four-dimensional data assimilation in a limited area
679 mesoscale model. Part I: experiments with synoptic-scale data, *Mon. Wea. Rev.*, 118, 1250-1277,
680 1990.

681

682 Stauffer, D. R., Seaman, N. L. and Binkowski, F. S.: Use of four-dimensional data assimilation in a
683 limited-area mesoscale model. Part II: effects of data assimilation within the planetary boundary layer,
684 *Mon. Wea. Rev.*, 119, 734-754, 1991.

685

686 Steele, C. J., Dorling, S. R., von Glasow, R. and Bacon, J.: Idealized WRF model sensitivity
687 simulations of sea breeze types and their effects on offshore windfields, *Atmos. Chem. Phys.*, 13, 443-
688 461, DOI: 10.5194/acp-13-443-2013, 2013.

689

690 Teo, C.-K., Koh, T.-Y., Lo, J. C.-F. and Bhatt, B. C.: Principal Component Analysis of observed and
691 modelled diurnal rainfall in the Maritime Continent, *J. Climate*, 24, 4662-4675, 2011.

692

693 Tetens, V.O.: Uber einige meteorologische. Begriffe, *Zeitschrift fur Geophysik*, 6, 297-309, 1930.

694

695 Waldron, K. M., Peagle, J. and Horel, J. D.: Sensitivity of a spectrally filtered and nudged limited area
696 model to outer model options, *Mon. Wea. Rev.*, 124, 529-547, 1996.

697

698 [Ummenhofer, C. C., England, M. H., McIntosh, P. C., Meyers, G. A., Pook, M. J., Risbey, J. S.,](#)
699 [Gupta, A. S. and Taschetto, A. S.: What causes Southeast Australia's worst droughts?, *Geophys. Res.*](#)
700 [Lett., 36\(4\), L04706, doi:10.1029/2008GL036801, 2009.](#)

701

702 von Storch, H., Langenberg, H. and Feser, F.: A spectral nudging technique for dynamical
703 downscaling purposes, *Mon. Wea. Rev.*, 128, 3664-3673, 2000.

704

705 Zeng, X. and Beljaars, A.: A prognostic scheme of sea surface skin temperature for modeling and data
706 assimilation, *Geophys. Res. Lett.*, 32, L14605, doi:10.1029/2005GL023030, 2005.